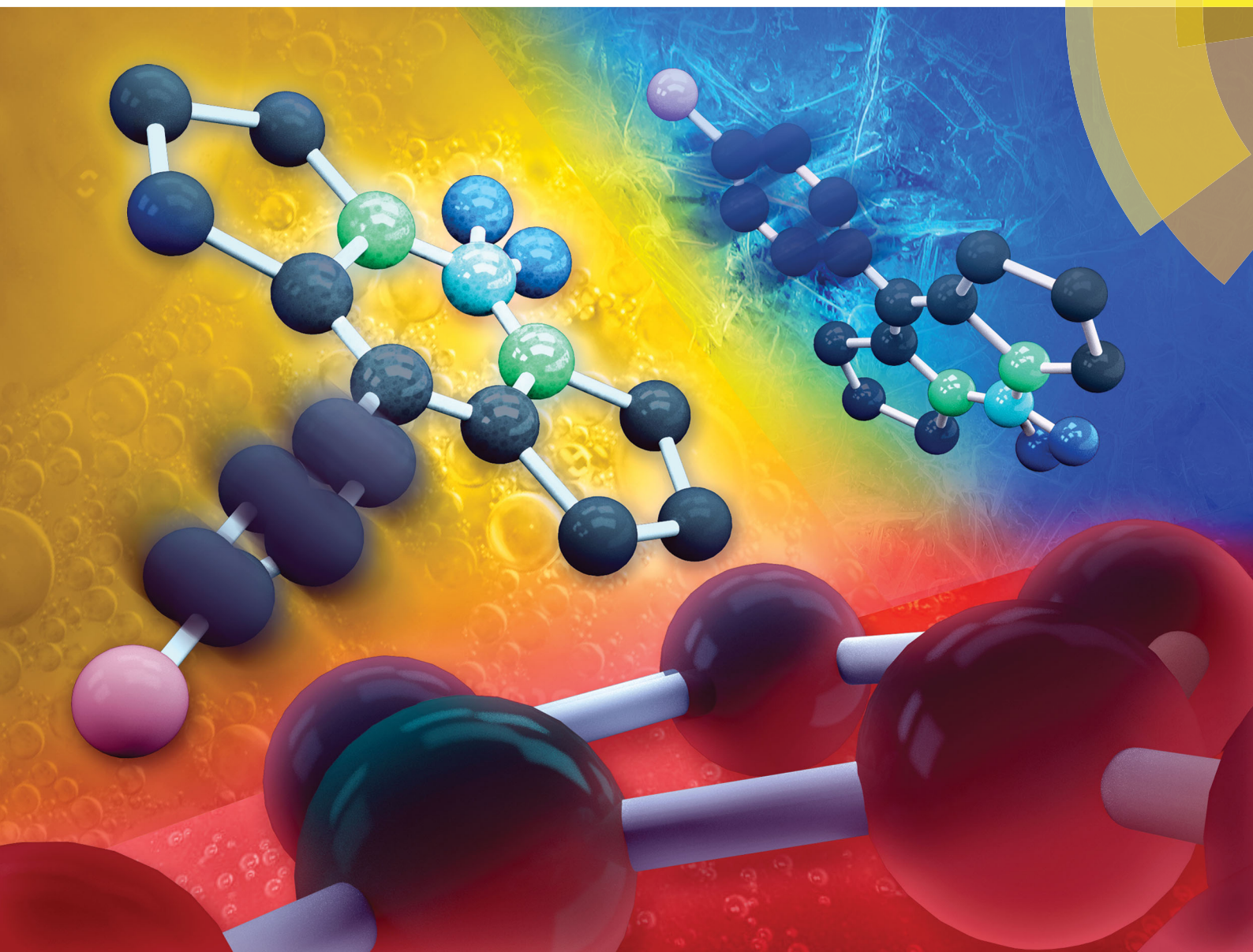


# PCCP

Physical Chemistry Chemical Physics

rsc.li/pccp



ISSN 1463-9076



**PAPER**

Marina K. Kuimova *et al.*

Exploring viscosity, polarity and temperature sensitivity of BODIPY-based molecular rotors

Cite this: *Phys. Chem. Chem. Phys.*,  
2017, **19**, 25252

# Exploring viscosity, polarity and temperature sensitivity of BODIPY-based molecular rotors†

Aurimas Vyšniauskas, ‡<sup>a</sup> Ismael López-Duarte, <sup>a</sup> Nicolas Duchemin,<sup>a</sup>  
Thanh-Truc Vu,<sup>a</sup> Yilei Wu,<sup>a</sup> Ekaterina M. Budykina,<sup>b</sup> Yulia A. Volkova,<sup>b</sup>  
Eduardo Peña Cabrera,<sup>c</sup> Diana E. Ramírez-Ornelas<sup>c</sup> and Marina K. Kuimova \*<sup>a</sup>

Microviscosity is a key parameter controlling the rate of diffusion and reactions on the microscale. One of the most convenient tools for measuring microviscosity is by fluorescent viscosity sensors termed 'molecular rotors'. BODIPY-based molecular rotors in particular proved extremely useful in combination with fluorescence lifetime imaging microscopy, for providing quantitative viscosity maps of living cells as well as measuring dynamic changes in viscosity over time. In this work, we investigate several new BODIPY-based molecular rotors with the aim of improving on the current viscosity sensing capabilities and understanding how the structure of the fluorophore is related to its function. We demonstrate that due to subtle structural changes, BODIPY-based molecular rotors may become sensitive to temperature and polarity of their environment, as well as to viscosity, and provide a photophysical model explaining the nature of this sensitivity. Our data suggests that a thorough understanding of the photophysics of any new molecular rotor, in environments of different viscosity, temperature and polarity, is a must before moving on to applications in viscosity sensing.

Received 26th May 2017,  
Accepted 6th July 2017

DOI: 10.1039/c7cp03571c

rsc.li/pccp

## Introduction

Molecular rotors are a class of viscosity-sensitive fluorescent compounds increasingly used as viscosity probes for micro-environments, which are inaccessible with traditionally used 'bulk' rheological methods.<sup>1–4</sup> Thus, molecular rotors have been successfully employed for measuring viscosity in lipid bilayers,<sup>5,6</sup> living cells,<sup>7–12</sup> atmospheric aerosols<sup>13,14</sup> and in polymer samples.<sup>15</sup> The origin of viscosity sensitivity in rotors is a conformational change that occurs in their excited state and leads to a formation of a 'dark state';<sup>1</sup> this conformational mobility can be impeded by higher viscosity. The lack of conformational change in a highly viscous environment results in an increase of fluorescence emission from a 'bright state'.

Consequently, molecular rotors have viscosity-dependent fluorescence spectra<sup>3,16</sup> and/or time-resolved fluorescence decays.<sup>7,8</sup> These viscosity-dependent properties have allowed quantitative

measurements of microviscosity using molecular rotors by ratiometric fluorescence intensity measurements<sup>3,17</sup> and by fluorescence lifetime imaging microscopy (FLIM).<sup>7,18</sup> The ratiometric or the FLIM-based detection is required in order to perform quantitative measurements of viscosity that are not biased by the variations in the concentration of the rotor, which cannot be easily determined in a heterogeneous microscopic environment, such as biological cells.

One of the most widely used viscosity sensors is the BODIPY-based molecular rotor **1** (Chart 1), which is characterised by viscosity-sensitive fluorescence decays, suitable for FLIM viscosity mapping. **1** has been shown to localize in the hydrophobic lipid tail region of a lipid bilayer<sup>6</sup> and it was previously used to measure viscosity in atmospheric aerosol particles,<sup>13,19</sup> during polymerisation,<sup>15</sup> as well as in model lipid membranes,<sup>5,6</sup> in protocells,<sup>20</sup> and in the inner membranes of a living cell.<sup>7</sup> One of the main advantages of **1** over other molecular rotors is its good dynamic range of fluorescence lifetimes, corresponding to a wide range of viscosities, and a very weak sensitivity to solvent polarity<sup>21</sup> and temperature.<sup>5</sup> Additionally, **1** offers facile and unambiguous interpretation of viscosity-sensitive data due to its monoexponential fluorescence decays,<sup>7</sup> which do not require a high number of photons to be collected. In addition to **1**, there has been a few other BODIPY-based viscosity probes with almost identical structure, with peripheral substitution of the core, and these dyes were used for viscosity sensing in lipid vesicles,<sup>22</sup> in a cell plasma membrane,<sup>23</sup> or for monitoring DNA interactions.<sup>24</sup>

<sup>a</sup> Chemistry Department, Imperial College London, Exhibition Road, SW7 2AZ, UK.  
E-mail: m.kuimova@imperial.ac.uk

<sup>b</sup> Department of Chemistry, Lomonosov Moscow State University, 119991, Russia

<sup>c</sup> Departamento de Química DCNE, Universidad de Guanajuato,  
Col. Noria Alta S/N, Guanajuato, Gto. 36050, Mexico

† Electronic supplementary information (ESI) available: Synthesis and characterization details for novel compounds and additional spectroscopic data. See DOI: 10.1039/c7cp03571c

‡ Present address: Center of Physical Sciences and Technology, Sauletekio av. 3, Vilnius, LT-10257, Lithuania.



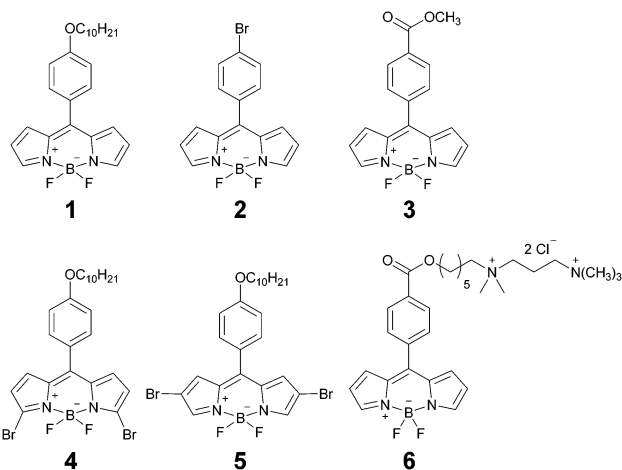


Chart 1 The molecular structures of the BODIPY-based molecular rotors.

In our recent work we have demonstrated that, unlike **1**, other molecular rotors can show a pronounced sensitivity to temperature,<sup>25</sup> which often cannot be decoupled from viscosity sensitivity, therefore, complicating their use as viscosity sensors. Moreover, on account of some charge transfer character in their 'dark' excited state, many molecular rotors are also sensitive to solvent polarity.<sup>26–28</sup> Taken together, these data suggest that the sensitivity to viscosity, temperature and polarity may be present in a single fluorescent sensor, which would complicate data interpretation and will render it less useful for sensing any of these individual environmental parameters. It follows that it is extremely important to thoroughly characterise any new molecular rotor at different temperatures and in solvents of different polarity. Unfortunately, this is not yet an established procedure when reporting new molecular rotors.

In this work we report an extended range of BODIPY-based molecular rotors (Chart 1), with the photophysical mechanism of viscosity sensitivity identical to **1**. We demonstrate that by making minor changes to the periphery of the sensor we are able to extend the dynamic range of viscosity sensitivity. At the same time, polarity or temperature sensitivity may result from these subtle substituent changes, ultimately resulting in an unusual interplay of viscosity, temperature and polarity sensitivity. We provide a photophysical model explaining such behaviour. Finally, we test the new molecular rotors in live cells.

## Methods

### BODIPY dyes and solvents

**1**,<sup>18</sup> **2**<sup>29</sup> and **3**<sup>30</sup> were synthesised as previously reported. The synthesis of previously unreported derivatives **4–6** is described in the ESI.† Stock solutions of all dyes were prepared in methanol (spectroscopic grade) at concentration of 1–5 mM and diluted for further experiments in a solvent or solvent mixtures of interest. All solvents used were of spectroscopic grade. Methanol, toluene and castor oil were obtained from Sigma-Aldrich. Glycerol was obtained from Alfa-Aesar. Viscosities of methanol–glycerol and toluene–castor oil mixtures at a variable temperature were

measured by the Stabinger viscometer (SVM3000, Anton Paar) with  $\pm 0.35\%$  accuracy.

### Absorption and fluorescence spectra

The Agilent 8453 UV-Vis spectrophotometer was used for measuring the absorption spectra. The fluorescence spectra were measured using the Fluoromax-4 spectrofluorometer (Jobin-Yvon, Horiba). The measurements were done in quartz cuvettes with the 10 mm path length. The concentration of the dyes was 2  $\mu\text{M}$ .

### Time-resolved fluorescence

The fluorescence decays of BODIPY dyes were measured using time-correlated single photon counting (TCSPC). The fluorescence decays of **1–5** in toluene–castor oil were measured using the in house TCSPC system composed of SPC-830 photon counting card (Becker & Hickl), DCC-100 detector control module (Becker & Hickl), PMC-100-1 PMT (Hamamatsu), Omni- $\lambda$  grating monochromator (LOT-Quantum Design), qpod cuvette holder (Quantum Northwest) and TC 125 Peltier temperature controller (Quantum Northwest). **1**, **4** and **5** were excited at 480 nm using the BDL-488-SMN picosecond diode laser (Becker & Hickl) at 20 MHz frequency. The acquisition time window was 50 ns, with 4096 collection channels. **2** and **3** were excited at 515 nm and 530 nm, respectively, using frequency-doubled Chameleon Vision II femtosecond Ti:sapphire laser (Coherent) at 80 MHz frequency. The acquisition time window was 12.5 ns, with 1024 collection channels. Fluorescence was detected at  $515 \pm 5$  nm (**1**),  $560 \pm 5$  nm (**2** and **3**),  $520 \pm 5$  nm (**4**),  $525 \pm 5$  nm (**5**). The instrument response function, which was required to fit the decays, was measured by recording a scattering signal from a cuvette with Ludox<sup>®</sup> solution.

### Imaging of live cells

Cell imaging experiments were done using SK-OV-3 human ovarian carcinoma cell line, obtained from ECACC. The cells were cultured in Dulbecco's modified Eagle's medium (DMEM) with 10% of foetal bovine serum (FBS). Cells were incubated at 37 °C, 5% of CO<sub>2</sub>. Before imaging, cells were seeded into 8-well Lab-Tek chamber slides for imaging and allowed to grow for 24 h. The seeding densities were 50 000 cells per well for the experiments with **2** and **3** and 20 000 cells per well for the experiments with **6**. For cell imaging with **2**, cells were kept in the 1  $\mu\text{M}$  solution of the dye in PBS for 1 min at 37 °C and then washed with PBS. Cells were incubated with **3** in Hank's Balanced Salt Solution (HBSS) at 3  $\mu\text{M}$  concentration at room temperature for 1 min. The incubation conditions for **6** were 13 min in HBSS without Ca<sup>2+</sup> and Mg<sup>2+</sup> ions with 44.5  $\mu\text{M}$  of **6** at 4 °C. FLIM imaging was done using Leica SP5-II microscope coupled with a SPC-830 photon counting card (Becker & Hickl). Two-photon excitation at 850 nm (**2**), 920 nm (**3**) and 800 nm (**6**) with Ti:Sapphire laser was used, and either a 40 $\times$  (HCX PL APO, N.A. – 0.85, Leica) or a 63 $\times$  objective (HCX PL APO water immersion, N.A. – 1.2, Leica). The fluorescence signal was detected over the 500–600 nm range. The FLIM image resolution was 256  $\times$  256 with 256 channels in time domain. IRF was measured by recording second harmonic generation (SHG) signal from urea.



## Data analysis

FLIM images were analysed using FLIMfit software developed at Imperial College London (v4.6.1).<sup>31</sup> Pixels were binned in order to have at least 1000 counts at the peak of the decay for reliable biexponential analysis. Intensity-weighted mean lifetimes were calculated for biexponential decays, which are defined as:

$$\bar{\tau} = \frac{\sum_i a_i \tau_i^2}{\sum_i a_i \tau_i}$$

where  $a_i$  and  $\tau_i$  are the amplitudes and the lifetimes of individual components. Fitting of fluorescence decays was done using a home-written code in MATLAB R2012a. The goodness of fit parameter ( $\chi_r^2$ ) was 1.2 or less for FLIM images and 1.5 or less for single decays. Further data processing and analysis was done with OriginPro 8.6.

## Results and discussion

### Probe design

Our probe design was based on the most successful rotor to date, structure **1** (Chart 1). We aimed to keep the photophysical mechanism of viscosity sensitivity of **1** by enabling an efficient rotation of the phenyl unit *versus* the BODIPY core. The ease of the phenyl group rotation in nonviscous solvents is thought to be responsible for the access to the dark non-emissive excited state, leading to efficient non-radiative decay.<sup>32</sup>

Our strategy was to test whether substitution on the phenyl unit may affect the photophysics of the rotors, Chart 1. Consequently, we introduced either the Br (**2**) or the ester (**3**) substituents to the *para*-position of the phenyl. Additionally, we have previously established that extended conjugation on the BODIPY core may lead to the temperature rather than viscosity sensitive behaviour.<sup>33</sup> Here, we introduced two symmetric Br substituents either on the alpha- (**4**) or the beta- (**5**) positions on the BODIPY core, in order to test the effect of this smaller non-conjugated substituent on the photophysical behaviour of the rotor. Finally, the derivative **6**, which can selectively stain the plasma membranes of live cells, was designed to be photophysically similar to **3**. The synthesis of all previously unreported derivatives is described in the ESI.†

### Photophysical characterisation

The absorption and fluorescence spectra of all dyes are typical of BODIPY fluorophores, with absorption maxima around 500 nm and emission maxima around 520 nm, Fig. S1 and Table S1 (ESI†). As expected, an addition of Br to the BODIPY core resulted in a small bathochromic shift of both absorption and fluorescence spectra, especially in the case of the beta-Br derivative **5**, which also displays broader spectra, compared to the unsubstituted BODIPY **1** or the alpha-Br derivative **4**.

The sensitivity of time resolved fluorescence decays of new derivatives **2** and **3** to viscosity was first tested in methanol–glycerol mixtures of varying viscosity, Fig. 1. Both dyes clearly showed good viscosity-sensitive response typical of molecular

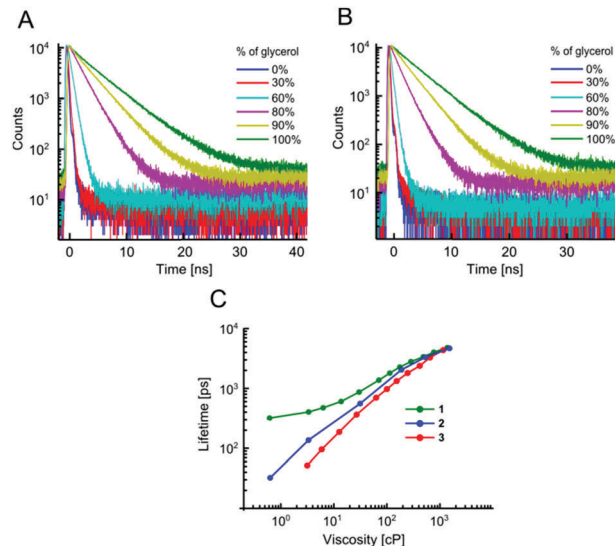


Fig. 1 The fluorescence decays of **2** (A) and **3** (B) in methanol–glycerol mixtures at 20 °C. (C) The fluorescence lifetimes of **2** (blue) and **3** (red) in methanol glycerol mixtures in comparison with the lifetimes of the previously reported molecular rotor **1**. Excitation and emission wavelengths were 480 nm and 520 nm, respectively.

rotors, with considerably longer decays observed in solutions of higher viscosity (higher glycerol content). These decays were fitted with an exponential decay function and this allowed the dependence of fluorescence lifetime on viscosity to be determined, Fig. 1C. The majority of fluorescence decays were monoexponential, but in the cases of biexponential decays, intensity-weighted mean lifetimes are shown, see Fig. S2, ESI† for further details of the biexponential fitting.

The results demonstrate that changing a substituent on the phenyl group in the *para* position does not prevent the dye from behaving as a molecular rotor. At the same time, it can dramatically tune its viscosity response. As could be seen from Fig. 1C, compared to the previously reported molecular rotor **1**, both **2** and **3** display a better dynamic range, with considerably higher sensitivity of lifetime to viscosity in a low viscosity range, 1–100 cP. While **1** is completely insensitive to viscosity below 10 cP, both **2** and **3** can be used in this range. Furthermore, the slope of the calibration curve (and therefore the sensitivity) of **2** and **3** are superior to **1** at viscosities below 100 cP. These results indicate that replacing the electron donating ether group on a phenyl unit in **1** with an electron withdrawing groups, such as a bromine atom (**2**), or an ester group (**3**), enhances the dynamic range of the BODIPY dyes as viscosity sensors.

We have previously demonstrated that **1** is not sensitive to temperature in methanol/glycerol mixtures, unlike several other dyes.<sup>25</sup> Next, we have tested the viscosity sensitivity of **2** and **3** in methanol–glycerol mixtures at various temperatures (Fig. 2A and C, solid circles). The bulk viscosities of these mixtures at multiple temperatures were measured by standard rheometry as explained in the Methods section. The lifetime data measured at different temperatures but at identical viscosities show a very close overlap, which means that the lifetimes of **2** and **3** are not



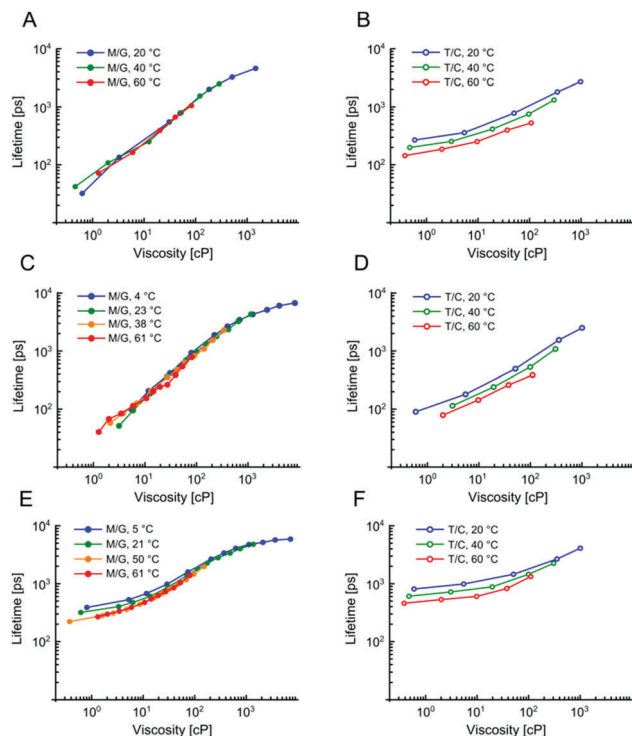


Fig. 2 The fluorescence lifetimes of **2** (A and B), **3** (C and D) and **1** (E and F) at different viscosities, temperatures and solvent polarities. The fluorescence lifetimes were measured in methanol–glycerol (A, C and E) and castor–toluene (B, D and F) mixtures. The results demonstrate that the dyes are affected not only by viscosity but by temperature and polarity as well.

sensitive to temperature, at least in methanol/glycerol mixtures. This is a desired property for a molecular rotor, since the sensitivity to both viscosity and temperature would require one of these two parameters to be kept constant throughout the experiment in order to measure the other.

**1** has been proven to be as a useful sensor for measuring viscosity in model lipid bilayers<sup>5,6</sup> and in the internal membranes of live cells.<sup>7</sup> We have previously shown that polarity does not affect the photophysical behavior of **1**, as long as the viscosity is above 70 cP,<sup>6</sup> which holds true for viscosities of most lipid bilayers, even those in the liquid disordered ( $L_d$ ) phase.

In order for **2** and **3** to be useful as lipid phase probes, they should ideally be calibrated in low polarity solvent mixtures, to keep the environment during the calibration as similar as possible to the viscosity measurement itself. Therefore, **2** and **3** were calibrated in non-polar toluene–castor oil mixtures at multiple temperatures. Additionally, **1** was calibrated in the same mixtures, for direct comparison. The results are shown in Fig. 2 and they reveal a very surprising and unexpected behaviour of dyes **2** and **3**. While for **1**, as previously reported, there is a good overlap between low and high polarity mixtures, above 80 cP, for **2** and **3** there is no overlap of calibration curves measured in methanol–glycerol (solid circles) and in toluene–castor oil (empty circles) mixtures. Additionally, we observed that for **2** and **3** the calibration curves measured in toluene–castor oil mixtures at different temperatures do not overlap. This means that both dyes are sensitive to polarity and correct calibration mixtures must be chosen to match the

polarity in a sample of interest. Additionally, both **2** and **3** are sensitive to temperature as well as to viscosity at low polarities. This is particularly surprising since **2** and **3** show no sensitivity to temperature in methanol–glycerol mixtures. Overall, all three dyes **1**, **2** and **3** show sensitivity to viscosity, temperature and polarity, at least to some extent, but the trends are very different for the three dyes, in spite of their structural similarity. Here, we propose a model that can explain these differences.

The key step leading to the function of rotors as viscosity sensors is their ability to rotate intramolecularly following excitation. Generally, a transition from a fluorescent state to a dark state is facilitated by such rotation. Consequently, viscosity affects the behavior of a molecule because it slows down the rotation. The rate of isomerisation can be expressed as:<sup>34</sup>

$$k_i = A(\eta)e^{-\frac{E_a}{kT}} \quad (1)$$

where  $k_i$  is the rate,  $A(\eta)$  is a viscosity-dependent preexponential factor,  $E_a$  is the energy of activation,  $k$  is the Boltzmann's constant and  $T$  is temperature. From eqn (1) it follows that the rotation can be sensitive to both viscosity and temperature in the presence of an activation energy barrier for intramolecular rotation. The rotors **2** and **3** show temperature-independent calibrations in methanol–glycerol mixtures but significant temperature sensitivity appears in toluene–castor oil mixtures. These data indicate that **2** and **3** have no such energy barrier in an environment of moderate-to-high polarity, however, a barrier appears in the low polarity environment, as shown in Fig. 3A. Interestingly, none of the dyes exhibit significant solvatochromism; the peaks in the absorption and fluorescence spectra get shifted by only  $\sim 7$  nm when the solvent is changed from methanol to toluene (Fig. S1 and Table S1, ESI†). This suggests that polarity mostly affects the dark state reached after the viscosity-dependent rotation instead of the bright fluorescent state.

In order to confirm this hypothesis, we derived an equation to correctly model the lifetime trends of all three BODIPY dyes. Fluorescence lifetime ( $\tau$ ) can be defined as follows:

$$\tau = \frac{1}{k_{\text{rot}}(\eta, T) + k_f + k_x} \quad (2)$$

where  $k_f$  is the rate constant of radiative decay,  $k_{\text{rot}}$  is the viscosity- and temperature-sensitive rate constant of the intramolecular rotation and  $k_x$  is the sum of any other rate constants that lead to the population loss from the fluorescent state of a molecular rotor.

The relationship between the quantum yield of fluorescence ( $\phi_f$ ) of a molecular rotor and viscosity was predicted by Förster and Hoffmann:<sup>35</sup>

$$\phi_f = C\eta^{-x} \quad (3)$$

where  $C$  and  $x$  are constants. The Förster–Hoffmann eqn (3) can be substituted into the preexponential factor  $A(\eta)$  in eqn (1) leading to:

$$k_{\text{rot}} = \frac{1}{C\eta^x + \frac{1}{A_{\text{max}}}} e^{-\frac{E_a}{kT}} \quad (4)$$



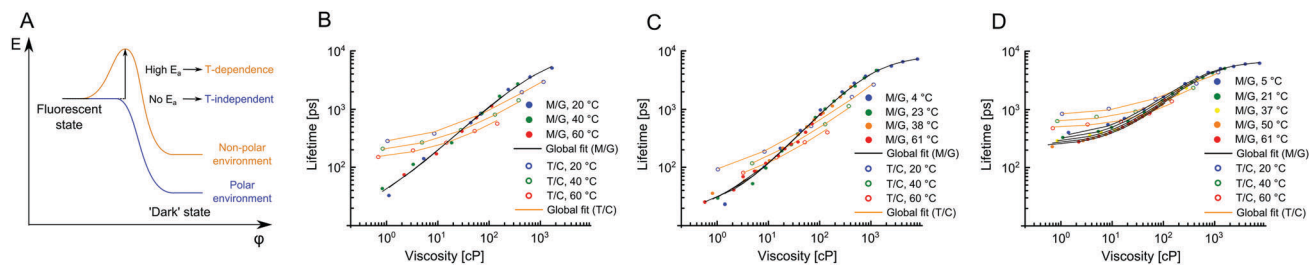


**Fig. 3** The photophysical model for BODIPY dyes **1–3** (A). The presence of an activation energy barrier is likely to give rise to the temperature dependence of the dye's lifetimes. (B–D) Global fits of lifetime data in Fig. 2 obtained using eqn (6), which was derived using the model shown in (A). For each dye methanol–glycerol (black) and toluene–castor oil (orange) datasets were fitted separately, resulting in 6 global fits in total. The data for dyes **2**, **3** and **1** are shown in (B), (C) and (D), respectively. The fitting parameters are given in Table S2, ESI.†

The term  $1/A_{\max}$  accounts for the fact that fluorescence lifetime does not go to zero at zero viscosity, but rather has a limit at low viscosities. At viscosity of 0 cP, the preexponential factor becomes equal to  $A_{\max}$ , which is the maximum achievable rate of the intramolecular rotation at zero viscosity and infinite temperature. Combining eqn (2) and (4) leads to the final equation describing how the lifetime of the molecular rotors depends on viscosity and temperature:

$$\tau = \frac{1}{\frac{1}{C\eta^x + \frac{1}{A_{\max}}} e^{-\frac{E_a}{kT}} + k_f + k_X} \quad (5)$$

The equation used to fit the lifetime data of **1**, **2** and **3** is:

$$\tau = \frac{1}{\frac{1}{a_1\eta^{a_2} + \frac{1}{a_3}} e^{\frac{a_4}{T}} + a_5} \quad (6)$$

where  $a_{1...5}$  are unconstrained fitting parameters. In total, six datasets (methanol–glycerol and toluene–castor oil datasets for each of the three dyes) were globally fitted using eqn (6) and the results are shown in Fig. 3. The fits demonstrate that eqn (6) correctly describes the behaviour of the three BODIPY-based molecular rotors. The fitting parameters are shown in Table S2, ESI.† The calculated activation energies (obtained from the parameter  $a_4$ ) were 0 for **2** and **3** in methanol–glycerol mixtures, 4.8 kJ mol<sup>-1</sup> for **1** in methanol–glycerol and 11 kJ mol<sup>-1</sup>, 12 kJ mol<sup>-1</sup> and 10 kJ mol<sup>-1</sup> for **1**, **2** and **3** in toluene–castor oil mixtures, respectively. As an attempt to create a single equation to globally fit the datasets measured in both methanol–glycerol and toluene–castor oil mixtures for each rotor we have expanded eqn (6) with additional empirical polarity-dependent terms (Fig. S3 and Table S3, ESI†). In order to fit the data we had to use polarity-dependent terms instead of constants  $a_1$ ,  $a_3$  and  $a_4$ , (eqn (6)). We emphasise that this expanded equation, while it allows to fit the data, is empirical in nature.

The behaviour of **2** and **3** exemplifies a potential pitfall with using molecular rotors without proper characterisation at different viscosities, temperatures and in solvent mixtures of different polarity. The fact that temperature sensitivity is “switched on” in low polarity environment can greatly complicate the interpretation of results, especially if the calibration

was done in methanol–glycerol mixtures only. We note that the model presented here was not based on any assumptions specific to BODIPY dyes and, as such, it is likely to hold true for any other molecular rotor.

In general, the presence of temperature sensitivity in a molecular rotor may be a more common occurrence than previously thought, due to a presence of an activation energy barrier for intramolecular rotation. Conversely, since the mechanism behind several fluorescent temperature sensors involves intramolecular rotation,<sup>36</sup> it is likely to be affected by viscosity. Therefore, the similarity in the mechanisms of temperature and viscosity-sensitivity of different groups of structurally flexible fluorophores might be greater than previously thought.

We have also attempted modifying **1** at the BODIPY core and synthesised dyes **4** and **5** with symmetrical Br substitution. The literature data for similar compounds in non-viscous solvents indicated that significant singlet oxygen production quantum yields (and hence the triplet state yields) are expected for both the alpha-Br and the beta-Br substitution of the BODIPY core.<sup>37</sup> At the same time, the fluorescence quantum yields in non-viscous solvents were not affected, compared to a non-substituted BODIPY.<sup>38</sup> To the best of our knowledge, the viscosity sensitivity of BODIPY dyes modified with Br substituents at the core was not previously investigated.

We have demonstrated that for both **4** and **5**, the Br modifications at the core greatly diminished molecular rotor properties, Fig. 4. The fluorescence decays remain monoexponential for **4** and **5** and the magnitude of fluorescence lifetimes at low viscosity (in methanol) is comparable to **1**, Fig. 4. However, it could be seen that the time-resolved fluorescence decays of **4** and **5** show only a weak dependence on viscosity, compared to **1**, Fig. 4. Overall, our results indicate that favourable tuning of the molecular rotor properties of BODIPY dyes is more readily achieved by synthetic modifications of the phenyl ring compared to modifying the core of BODIPY. The modifications of the phenyl ring is also more readily achieved synthetically.

### Cellular imaging

Our data indicate that the new derivatives **2** and **3** possess the widest calibration range of lifetime vs. viscosity, and can be used for quantitative measurements, if the polarity of the environment is known. We have also synthesised derivative **6**,



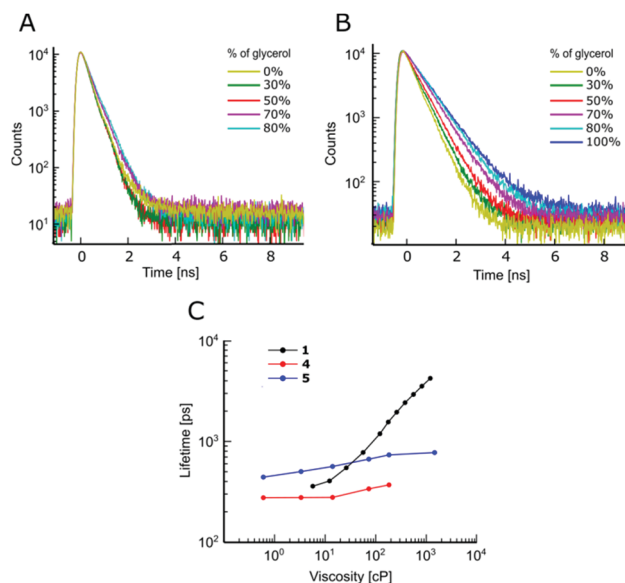


Fig. 4 The time resolved fluorescence decays of **4** (A) and **5** (B) obtained in methanol–glycerol mixtures at 20 °C. Excitation and emission wavelengths were 480 nm and 520 nm, respectively. (C) The lifetime/viscosity calibration curves for **1**, **4** and **5**.

which was expected to be very close photophysically to **3** (*i.e.* should possess a high dynamic range of viscosity). In addition, the rotor **6** also had necessary functional groups to enable the staining of cellular plasma membrane, by analogy to our previously published design.<sup>23</sup> We tested **2**, **3** and **6** in live epithelial cells, Fig. 6.

All three dyes successfully stained the cells, with **2** and **3** showing effective endocytosis and internalisation, similarly to **1**, while **6** showed good plasma membrane staining, analogously to previously reported BODIPY-ether derivative with a double charge on its tail.<sup>23</sup> **6** shows minimal sensitivity to temperature in methanol–glycerol mixtures (Fig. 5A), similar to **3**. Also, we have verified that **6** has a nearly identical lifetime/viscosity calibration to **3**, at least in methanol/glycerol solutions, Fig. 5B. Similarly to **3**, we detected an improved dynamic range, allowing the measurements of viscosity < 100 cP with **6**. Due to its charged nature, **6** was not soluble in toluene–castor oil mixtures. Given nearly identical photophysical properties of **3** and **6** in methanol–glycerol, Fig. 5B, the viscosities for **6** in cells were assigned using data of **3** in toluene–castor oil mixtures.

Next we performed FLIM measurements on cells containing **2**, **3** and **6**. It should be noted that, due to longer acquisition times required for **6**, a significant internalisation of the dye was observed and FLIM images did not have exclusive membrane staining. In all FLIM images, fluorescence decays for **2**, **3** and **6** were biexponential. It is well known that for BODIPY-based dyes the presence of a biexponential decay can be a hallmark of dye aggregation<sup>5</sup> with aggregated species characterised by a weak emission band centred at 650–700 nm. Aggregate formation results in the quenching of the main emission band centered at 515 nm<sup>5</sup> which renders the lifetime–viscosity calibration curve unusable. We have recorded time resolved decays from cells for

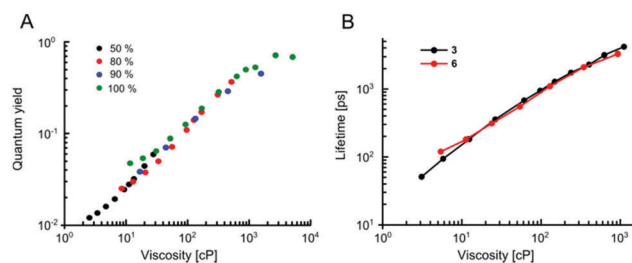


Fig. 5 (A) The lifetimes of **6** in methanol–glycerol mixtures at 3–100 °C temperatures. (B) The fluorescence lifetimes of dyes **3** and **6** in methanol–glycerol mixtures at room temperature. The calibration curves are identical within measurement error and suggest identical photophysical properties of **3** and **6**.

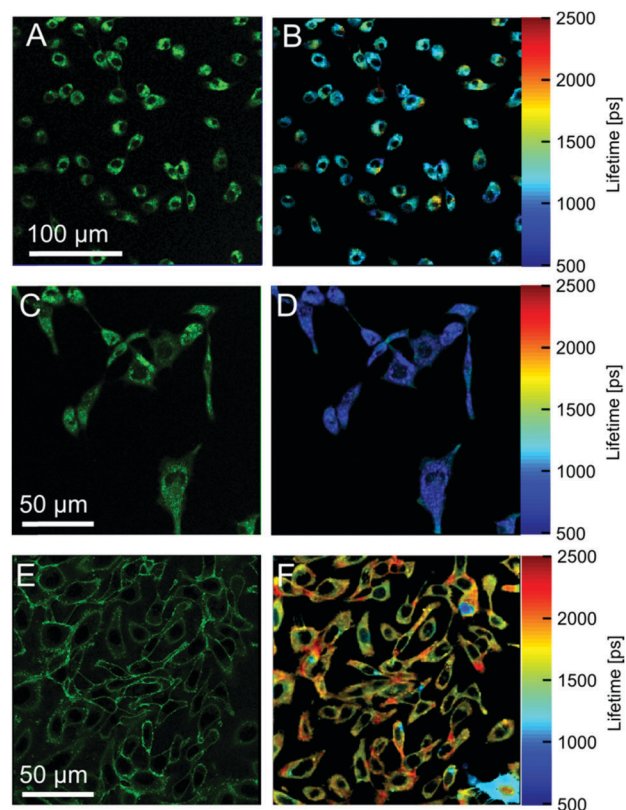


Fig. 6 Fluorescence images of dyes **2** (A) **3** (C) and **6** (E) in SK-OV-3 cells. Membrane staining is achieved only with the dye **6**. The right column shows FLIM images obtained using **2** (B), **3** (D) and **6** (F).

all dyes in two spectral windows: for monomers (500–600 nm) and aggregates (600–650 nm), Fig. S4, ESI.† We found that the monomer/aggregate traces for all three dyes were close to identical. This means that likely no aggregates are present and the lifetime values are likely to correspond to two environments of different viscosity detected in cells, although a small possibility that aggregation of the rotors played some role in the observed FLIM signatures cannot be excluded.

The lifetimes of **2** were 562 ps and 2023 ps with amplitudes of 78% and 22%. The lifetimes correspond to viscosities of ~ 20 cP and ~ 450 cP assigned using the calibration data in toluene–castor



oil at 20 °C (Fig. 2A). The lifetimes of **3** were 452 ps and 1518 ps with corresponding amplitudes of 81% and 19%. These lifetimes correspond to ~50 cP and ~420 cP viscosities, which were assigned using calibration data of **3** in toluene–castor oil mixtures at 20 °C. The data for **6** were 238 ps and 2205 ps with amplitudes of 75% and 25%, respectively, corresponding to viscosities of ~20 cP and ~800 cP. Thus, the viscosities determined by the rotors **3** and **6** in cells are quite different, which suggests that **3** and **6** take up different locations inside membranes. Another possibility is that the ester bond of **6** can be cleaved intracellularly by esterases. This can explain the fast internalization of this dye in cells, compared to the previously reported ether derivative of **1**.<sup>23</sup>

Overall, we have shown that the dyes **2**, **3** and **6** stained the cells successfully, although biexponential character of the fluorescence decays complicate unambiguous assignment of viscosity values. Our results illustrate that one of the main sought-after properties of new molecular rotors should be the monoexponential decay kinetics, which greatly simplifies their application. In that respect, and coupled with excellent stability in the biological environment, BODIPY **1** and its derivatives remain the golden standard of cellular imaging of local viscosity.<sup>7,23,39,40</sup>

## Conclusions

To conclude, we have synthesised and tested a series of new BODIPY-based molecular rotors. We have found that replacing the electron donating ether group in a widely used derivative **1** with the weakly electron withdrawing bromine atom (**2**) or the ester group (**3**) significantly improved the dynamic range of viscosity sensing in a molecular rotor. We have also discovered that the modifications of the BODIPY core with bromine atoms almost completely eliminated the sensitivity to viscosity. Most importantly, by thoroughly testing all new molecular rotors in solvent mixtures of different viscosity and polarity at different temperatures, we have shown that molecular rotors can be affected by all three environmental parameters: viscosity, temperature and polarity. We have provided the photophysical model explaining this complex behaviour that fully described the photophysical data of the molecular rotors. Furthermore, our proposed model is likely to be applicable to any molecular rotor, and can be used to estimate crucial photophysical parameters from the measured time resolved data. Finally, the new molecular rotors were tested in live cells. Overall, our results demonstrate the importance of thorough calibration of molecular rotors at different viscosity, temperature and polarity and broaden our understanding of molecular rotors in general.

## Acknowledgements

AV thanks the EPSRC for the Doctoral Prize Fellowship. MKK is thankful to the EPSRC for the Career Acceleration Fellowship (EP/I003983/1). We are thankful to Imperial College Global Engagements EPSRC fund for the travel grants to EMB and YEV. This work was partially supported by the European Commission in the form of Marie Curie individual Fellowship to TTV.

## Notes and references

- M. A. Haidekker, M. Nipper, A. Mustafic, D. Lichlyter, M. Dakanali and E. A. Theodorakis, *Dyes with Segmental Mobility: Molecular Rotors*, Springer Berlin Heidelberg, Berlin, Heidelberg, 2010, vol. 8.
- M. K. Kuimova, *Phys. Chem. Chem. Phys.*, 2012, **14**, 12671–12686.
- M. K. Kuimova, S. W. Botchway, A. W. Parker, M. Balaz, H. A. Collins, H. L. Anderson, K. Suhling and P. R. Ogilby, *Nat. Chem.*, 2009, **1**, 69–73.
- M. A. Haidekker and E. A. Theodorakis, *Org. Biomol. Chem.*, 2007, **5**, 1669–1678.
- Y. Wu, M. Stefl, A. Olżyńska, M. Hof, G. Yahioglu, P. Yip, D. R. Casey, O. Ces, J. Humpolíčková and M. K. Kuimova, *Phys. Chem. Chem. Phys.*, 2013, **15**, 14986–14993.
- M. R. Dent, I. Lopez Duarte, C. J. Dickson, N. D. Geoghegan, J. M. Cooper, I. R. Gould, R. Krams, J. A. Bull, N. J. Brooks and M. K. Kuimova, *Phys. Chem. Chem. Phys.*, 2015, **17**, 18393–18402.
- M. K. Kuimova, G. Yahioglu, J. A. Levitt and K. Suhling, *J. Am. Chem. Soc.*, 2008, **130**, 6672–6673.
- X. J. Peng, Z. G. Yang, J. Y. Wang, J. L. Fan, Y. X. He, F. L. Song, B. S. Wang, S. G. Sun, J. L. Qu, J. Qi and M. Yang, *J. Am. Chem. Soc.*, 2011, **133**, 6626–6635.
- Z. Yang, Y. He, J. H. Lee, W.-S. Chae, W. Ren, J. H. Lee, C. Kang and J. S. Kim, *Chem. Commun.*, 2014, **50**, 11672–11675.
- Z. Yang, Y. He, J.-H. Lee, N. Park, M. Suh, W.-S. Chae, J. Cao, X. Peng, H. Jung, C. Kang and J. S. Kim, *J. Am. Chem. Soc.*, 2013, **135**, 9181–9185.
- E. Gatzogiannis, Z. Chen, L. Wei, R. Wombacher, Y.-T. Kao, G. Yefremov, V. W. Cornish and W. Min, *Chem. Commun.*, 2012, **48**, 8694–8696.
- L. Wang, Y. Xiao, W. Tian and L. Deng, *J. Am. Chem. Soc.*, 2013, **135**, 2903–2906.
- N. A. Hosny, C. Fitzgerald, A. Vyšniauskas, T. Athanasiadis, T. Berkemeier, N. Uygur, U. Pöschl, M. Shiraiwa, M. Kalberer, F. D. Pope and M. K. Kuimova, *Chem. Sci.*, 2016, **7**, 1357–1367.
- T. Athanasiadis, C. Fitzgerald, N. Davidson, C. Giorio, S. W. Botchway, A. D. Ward, M. Kalberer, F. D. Pope and M. K. Kuimova, *Phys. Chem. Chem. Phys.*, 2016, **18**, 30385–30393.
- J. M. Nölle, C. Jüngst, A. Zumbusch and D. Wöll, *Polym. Chem.*, 2014, **5**, 2700–2703.
- M. A. Haidekker, T. P. Brady, D. Lichlyter and E. A. Theodorakis, *J. Am. Chem. Soc.*, 2006, **128**, 398–399.
- A. Vyšniauskas, M. Balaz, H. L. Anderson and M. K. Kuimova, *Phys. Chem. Chem. Phys.*, 2015, **17**, 7548–7554.
- J. A. Levitt, M. K. Kuimova, G. Yahioglu, P. H. Chung, K. Suhling and D. Phillips, *J. Phys. Chem. C*, 2009, **113**, 11634–11642.
- N. A. Hosny, C. Fitzgerald, C. Tong, M. Kalberer, M. K. Kuimova and F. D. Pope, *Faraday Discuss.*, 2013, **165**, 343–356.
- T.-Y. Dora Tang, C. Rohaida Che Hak, A. J. Thompson, M. K. Kuimova, D. S. Williams, A. W. Perriman and S. Mann, *Nat. Chem.*, 2014, **6**, 527–533.



- 21 J. A. Levitt, P.-H. Chung, M. K. Kuimova, G. Yahioğlu, Y. Wang, J. Qu and K. Suhling, *ChemPhysChem*, 2011, **12**, 662–672.
- 22 M. Olšínová, P. Jurkiewicz, M. Pozník, R. Sachl, T. Prausová, M. Hof, V. Kozmík, F. Teplý, J. Svoboda and M. Cebeacauer, *Phys. Chem. Chem. Phys.*, 2014, **16**, 10688–10697.
- 23 I. López-Duarte, T. T. Vu, M. A. Izquierdo, J. A. Bull and M. K. Kuimova, *Chem. Commun.*, 2014, **50**, 5282–5284.
- 24 D. Dziuba, P. Jurkiewicz, M. Cebeacauer, M. Hof and M. Hocek, *Angew. Chem., Int. Ed.*, 2016, **55**, 174–178.
- 25 A. Vyšniauskas, M. Qurashi, N. Gallop, M. Balaz, H. L. Anderson and M. K. Kuimova, *Chem. Sci.*, 2015, **6**, 5773–5778.
- 26 M. A. Haidekker, T. P. Brady, D. Lichlyter and E. A. Theodorakis, *Bioorg. Chem.*, 2005, **33**, 415–425.
- 27 N. Jiang, J. Fan, S. Zhang, T. Wu, J. Wang, P. Gao, J. Qu, F. Zhou and X. Peng, *Sens. Actuators, B*, 2014, **190**, 685–693.
- 28 M. R. Dent, I. López-Duarte, C. J. Dickson, P. Chairatana, H. L. Anderson, I. R. Gould, D. Wylie, A. Vyšniauskas, N. J. Brooks and M. K. Kuimova, *Chem. Commun.*, 2016, **52**, 13269–13272.
- 29 E. Pena-Cabrera, A. Aguilar-Aguilar, M. Gonzalez-Dominguez, E. Lager, R. Zamudio-Vazquez, J. Godoy-Vargas and F. Villanueva-Garcia, *Org. Lett.*, 2007, **9**, 3985–3988.
- 30 A. Cui, X. Peng, J. Fan, X. Chen, Y. Wu and B. Guo, *J. Photochem. Photobiol., A*, 2007, **186**, 85–92.
- 31 S. C. Warren, A. Margineanu, D. Alibhai, D. J. Kelly, C. Talbot, Y. Alexandrov, I. Munro, M. Katan, C. Dunsby and P. M. W. French, *PLoS One*, 2013, **8**, e70687.
- 32 F. Li, S. I. Yang, Y. Ciringh, J. Seth, C. H. Martin, D. L. Singh, D. Kim, R. R. Birge, D. F. Bocian, D. Holten and J. S. Lindsey, *J. Am. Chem. Soc.*, 1998, **120**, 10001–10017.
- 33 T. T. Vu, R. Méallet-Renault, G. Clavier, B. A. Trofimov and M. K. Kuimova, *J. Mater. Chem. C*, 2016, **4**, 2828–2833.
- 34 S. P. Velsko and G. X. Fleming, *Chem. Phys.*, 1982, **65**, 59–70.
- 35 T. Forster and G. Hoffmann, *Z. Phys. Chem.*, 1971, **75**, 63–76.
- 36 K. Casey and E. Quitevis, *J. Phys. Chem.*, 1988, **92**, 6590–6594.
- 37 A. J. Sánchez-Arroyo, E. Palao, A. R. Agarrabeitia, M. J. Ortiz and D. García-Fresnadillo, *Phys. Chem. Chem. Phys.*, 2017, **19**, 69–72.
- 38 V. Lakshmi and M. Ravikanth, *Dalton Trans.*, 2012, **41**, 5903–5911.
- 39 J. T. Mika, A. J. Thompson, M. R. Dent, N. J. Brooks, J. Michiels, J. Hofkens and M. K. Kuimova, *Biophys. J.*, 2016, 1528–1540.
- 40 L. E. Shimolina, M. A. Izquierdo, I. López-Duarte, J. A. Bull, M. V. Shirmanova, L. G. Klapshina, E. V. Zagaynova and M. K. Kuimova, *Sci. Rep.*, 2017, **7**, 41097.

